Comparative Study of the Thermal Behaviors of a Cement Mortar Wall Including Bio-based Microencapsulated Phase Change Materials and a Reference Wall

Franck Komi Gbekou[1(✉)], Abderrahim Boudenne[2], Anissa Eddhahak[3], and Karim Benzarti[1(✉)]

[1] Univ Gustave Eiffel, Ecole des Ponts, CNRS, Navier, 77447 Marne la Vallée, France
{komi.gbekou,karim.benzarti}@univ-eiffel.fr
[2] Univ Paris Est Créteil, CERTES, 94010 Créteil, France
[3] Arts et Métiers ParisTech, PIMM, 75013 Paris, France

Abstract. This study aims to evaluate the thermal behavior of a cement mortar wall (denoted M15D) including bio-based microencapsulated phase change materials (mPCMs) in comparison to a reference wall without mPCMs (M0). A bi-climatic test setup was designed and built in order to submit the two sides of the walls to different hygrothermal conditions representing the outdoor and indoor environments. Two scenarios were considered for the outdoor conditions: a cyclic solicitation of 12 h at 40 °C followed by 12 h at 15 °C to simulate a day/night variation, and a step change from 20 °C to 40 °C followed by prolonged exposure at 40 °C until steady-state, both at fixed relative humidity (50% RH). Temperature sensors installed at different depths made it possible to monitor temperature gradients within the walls during the tests. Overall, quite similar responses were collected for the two walls exposed to the same outdoor scenario. However, the maximum temperatures recorded on the external face and at several depth locations were slightly lower for the M15D wall compared to M0, with a gap of about 1 °C. This result suggests that the incorporation of mPCMs in the wall may contribute to dampen the effect of external temperature variations, although this action remains limited. Furthermore, this bio-based mPCM system offers an environmentally friendly alternative to traditional paraffinic mPCMs.

Keywords: bio-based microencapsulated phase change materials (mPCMs) · heat transfer · bi-climatic setup · wall-scale study

1 Introduction

In the current context of global warming, the reduction of both energy consumption and CO_2 emissions has become a major challenge for our modern societies [1]. The building and construction sector is responsible for about 30% of the total energy consumption in France [2], and most part of this energy is used to maintain living comfort (electricity, air conditioning, heating). To reduce this impact, public policies encourage the development

S. Amziane et al. (Eds.): ICBBM 2023, RILEM Bookseries 45, pp. 817–828, 2023.
https://doi.org/10.1007/978-3-031-33465-8_63

of innovative solutions capable of improving the thermal efficiency of buildings [1, 3]. Therefore, significant research is being dedicated to the design of construction materials with improved thermal properties, and preferably including bio-based components to provide more environmentally friendly alternatives [4–6].

Latent heat thermal energy storage systems are considered as a promising approach [7]. These systems allow the storage of certain quantity of energy that can be released later to meet specific needs [6, 8]. They include phase change materials (PCM), which have the ability to changes their physical state (e.g. solid to liquid) upon temperature variations and store/release energy during phases changes [9, 10]. The combination of PCMs (in the form of macro or micro encapsulated materials) with conventional buildings materials like mortar or concrete, has been investigated in many studies and has given promising results, as it resulted in significant improvement in thermophysical properties [11–14]. Studies at larger scales (wall and building scale) have been also carried-out to evaluate the effective gain in thermal performance following the incorporation of PCM into mortars. In general, these studies mainly focused on the use of PCM layers in multi-layered insulation systems. Li et al. [15], showed for instance that the addition of an insulating layer with PCMs to a cementitious mortar wall, allows to attenuate the indoor/outdoor temperature difference in a room and to increase energy saving rates up to 30%.

To the best of our knowledge, most systems are multi-layered and the hygrothermal performance of a thick and homogeneous cement mortar wall including microencapsulated PCMs (mPCMs) has not been investigated so far. Therefore, this study aims to compare the thermal responses of a homogeneous mortar wall incorporating bio-based and formaldehyde-free mPCMs, and a reference wall made of regular mortar, in order to evaluate the gain in performance resulting from mPCM addition. Both walls were tested with a home-made bi-climatic setup, in which the wall sides are exposed to specific hygrothermal conditions representing the outdoor and indoor environments. Temperature variations were recorded at different depth of the wall during testing, in order to determine the global thermal behavior of each wall and discuss the possible effect of mPCM incorporation.

2 Materials and Experimental Methods

2.1 Materials

The study involved two cement mortar walls: one reference wall made of regular mortar, and a second wall including microencapsulated phase change materials (mPCMs). The reference mortar (denoted M0) is an existing formulation from the literature [16] and contains: an ordinary Portland cement EXTREMAT® CEM I 52.5 N (denoted OPC), a fast-setting Sulfo-aluminous cement Alpenat R^2 (denoted CSA), both manufactured by VICAT company (L'Isle-d'Abeau, France), a superplasticizer (SP)/water reducer VISCOCRETE TEMPO 11 from SIKA (Baar, Switzerland), standardized sand with a maximum diameter of 2 mm provided by Société Nouvelle du Littoral (Leucate, France). The composition of the reference mortar M0 is detailed in Table 1.

The mPCM used is a commercial product (CrodaTherm™ ME29D), supplied in the form of an aqueous dispersion of microencapsulated particles in water (solid content

of about 50 wt.%). The particles consist of an organic PCM core derived from plant-based feedstocks, surrounded by an acrylic polymer, and display maximum melting and crystallization temperatures of 28.8 °C and 23.5 °C, respectively, and heats of fusion and crystallization of 183 kJ/kg and −179 kJ/kg, according to the product datasheet [17]. Such a liquid dispersion was chosen because it can be easily incorporated into the cement mortars at an early stage of the mixing process (together with the mixing water). In addition, CrodaTherm™ ME29D is certified bio-based and formaldehyde free, which ensures both reduced environmental footprint and low safety/health hazard.

A preliminary material-scale study was conducted regarding the incorporation of these mPCMs into the reference mortar M0 and its influence on the mechanical and thermophysical properties of the resulting materials [11]. This study, carried out on several mortars with mPCM contents in the range 0–13.5 wt.%, made it possible to highlight significant improvement in thermal properties upon mPCM addition, but at the expense of mechanical performance. Introducing 11.03 wt.% of mPCM in the mortar was found to reduce the thermal conductivity by 72% (0.6 $W.m^{-1} \cdot K^{-1}$ compared to 2.3 $W.m^{-1} \cdot K^{-1}$ for M0), while still providing an acceptable compressive strength of 12 MPa. This formulation, denoted M15D, was thus selected to conduct a study at the wall scale, with the objective to compare the thermal responses of a wall made of the reference mortar M0, and another wall based on this M15D formulation. The composition of mortar M15D is also summarized in Table 1.

Table 1. Composition of the two mortar formulations used in this work.

Type of mortar	Sand (g)	OPC (g)	CSA (g)	SP (g)	Mass of mPCM particles (g)	Total water (g)	W/C ratio	Weight fraction of mPCM particles (%)	Volume fraction of mPCM particles (%)
M0	1350	1059.33	79.73	2.96	–	398.67	0.35	0	0
M15D	1350	1059.33	79.73	2.96	433.06	1006.2	0.88	11.03	20.94

2.2 Determination of the Thermophysical Properties of the Mortars

The thermophysical properties of the two mortars M0 and M15D were determined using the Hot Disk method (denoted HD) with a TPS 2500 S device from Hot Disk Company (Gothenburg, Sweden). The sensor used was a "Kapton insulated" model (ref 5501) from Hot Disk® with a radius of 6.4 mm. The HD enables a fast, non-destructive and accurate measurement of the thermal conductivity (λ in $W.m^{-1} \cdot K^{-1}$), the thermal diffusivity (α in $m^2 \cdot s^{-1}$), and the volumetric heat capacity ($\rho.Cp$ in $MJ.m^{-3} \cdot K^{-1}$). The sensor is placed between two samples of the same material, and acts both as a heat source to increase the sample's temperature and as a resistance thermometer to record the time-dependent increase in temperature. To ensure reproducible conditions, measurements were carried out in a controlled climatic chamber at a constant relative humidity of 50%

and over a temperature range from 10 °C to 45 °C to cover the entire phase change domain the mPCMs.

2.3 Experimental Setup for Bi-climatic Wall Test

The Bi-climatic Experimental Setup

A specific setup was designed for the experiment. The objective is to simulate a bi-climatic environment by submitting the wall sides to two different hygrothermal conditions representing the outdoor and indoor environments.

The bi-climatic system combines a climatic chamber (Memmert ICH 260, whose door has been removed) and a metallic frame designed to support the wall and connect this latter to the chamber. The whole device is installed in a laboratory at controlled temperature (20 °C). The climatic chamber allows to simulate the outdoor environment by applying dynamic temperature cycles on the outer face of the wall, while the other face is exposed to the laboratory condition that simulates the indoor environment of a building.

The metallic frame is fixed to the chamber and a 6 cm thick insulation material is placed in-between to insulate the borders of the central open area (40 cm × 45 cm), so that thermal exchanges between the chamber and the wall can only occurs through this open area. The insulation material is then completely covered with an insulating and vapor barrier adhesive plastic film (Fig. 1).

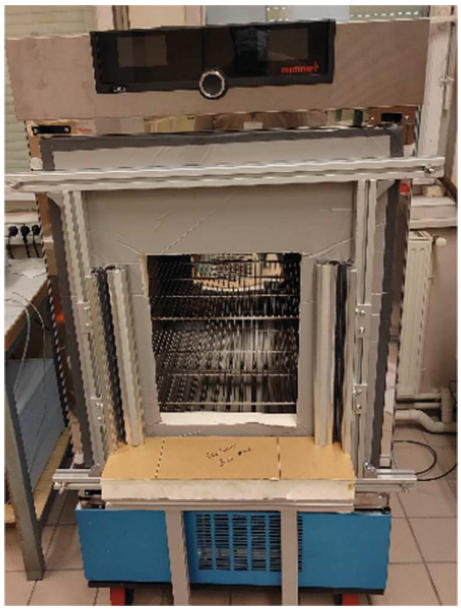

Fig. 1. Picture of the climatic chamber and the designed frame's structure

Preparation and Instrumentation of the Walls

The two mortar formulations M0 and M15D were prepared according to the mixing procedure detailed in a previous article [11]. Walls of dimensions 50 × 50 × 10 cm^3 were then manufactured by casting the fresh mortar mixes in wood formworks. They were demolded after about one week, and were cured for several months in the laboratory at 20 °C and ambient hygrometry, so that the microstructure of the cement matrix is almost stabilized.

The walls were then instrumented with temperature sensors. 3 holes of depth 25 cm were drilled in the thickness of the wall, at distances of 2.5 cm, 5 cm and 7.5 cm respectively from the outer face (Fig. 2), and using a column drilling machine to ensure precise vertical drilling (Fig. 3). The holes were vertically spaced 15 cm from each other to avoid any disturbance on sensor's measurements (Fig. 2).

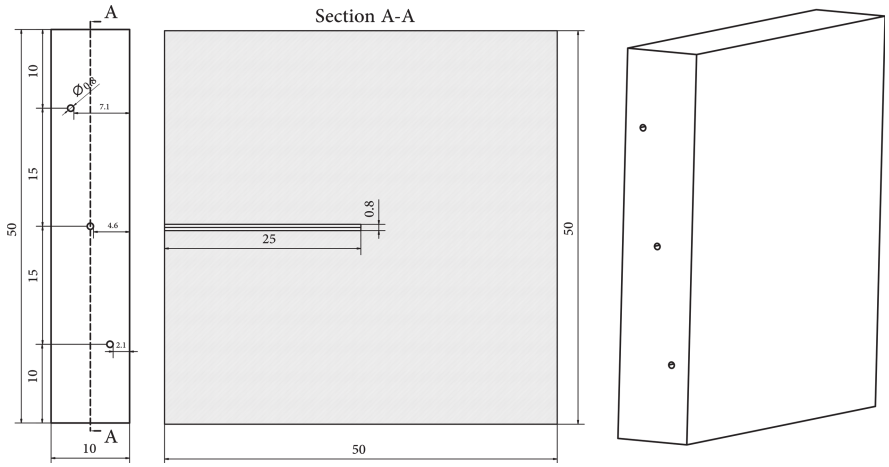

Fig. 2. Locations of holes for the insertion of temperature sensors at different depths of the wall

A total of five sensors were installed on each wall (Fig. 3), three in the thickness and one on each face to record temperature variations at different depths. All lateral faces were insulated with expanded polystyrene, to force unidirectional (1D) thermal transfer to occur through the two exposed surfaces only. In addition, two other sensors are placed in the climatic chamber and in the laboratory to record indoor and outdoor temperature conditions.

Finally, a thermal camera was used to check the quality of the setup insulation, in order to prevent possible heat loss and ensure uniform heat transfer across the observed surface.

Temperature Cycles

After the setup configuration, the wall was pre-conditioned by setting the climatic chamber at 20 °C and 50% RH, until all the sensors provide a stabilized temperature (for

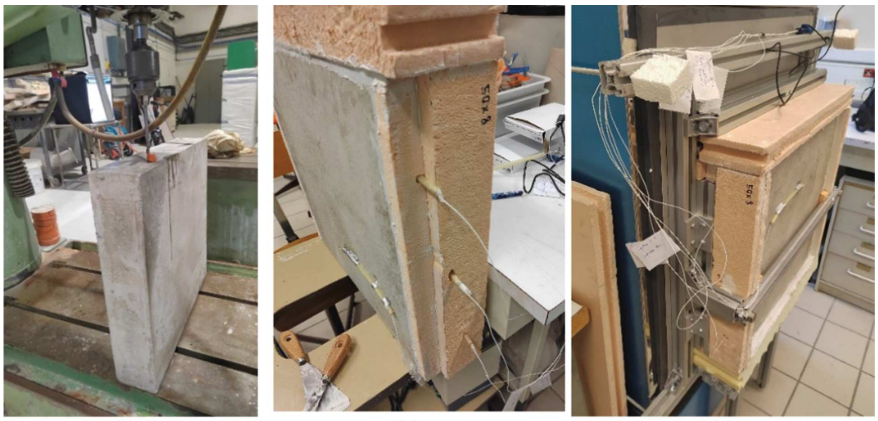

(a) (b) (c)

Fig. 3. Preparation of the wall: (a) drilling stage, (b) sensors' introduction, (c) final setup.

about one week). The dynamic temperature cycles were then programmed on the climatic chamber using Atmo-Control (control software of the Memmert chamber). Two experimental programs were applied to the walls, both at fixed humidity level (50% RH):

- A cyclic temperature program which consists in exposing the wall to a period of 12 h at 40 °C, followed by 12 h at 15 °C, representative of a day/night alternation.
- An initial step change from 20 °C to 40 °C, followed by a prolonged exposure at 40 °C until reaching a steady-state regime.

3 Results

3.1 Thermophysical Properties of the Two Mortars

Thermophysical properties of the two mortars M0 and M15D measured with the HD method at different temperatures are presented in Fig. 4.

The mortar filled with 11.03 wt.% of mPCMs exhibits much lower values of the three measured properties compared to the reference material, whatever the temperature considered. For example, the thermal conductivity at 20 °C is reduced by ~72%, from 2.32 $W.m^{-1} \cdot K^{-1}$ to 0.66 $W.m^{-1} \cdot K^{-1}$. This drop can be explained by the low thermal conductivity of the mPCMs (0.25–0.35 $W.m^{-1} \cdot K^{-1}$ depending on the physical state of the PCM core) [11], and by the large increase in porosity of the mortar which favors thermal transfer by convection in the pores instead of thermal conduction [18–20]. This result is consistent with the observations of Dehdezi *et al.* [18], Hunger et *al.* [19], and Jayalath *et al.* [20]. These authors reported respective decreases in thermal conductivity of ~36%, ~38%, and ~45% with the addition of 5 wt.% mPCMs into cement composites, compared to reference specimens.

3.2 Comparison of the Walls' Behaviors Under Heating/cooling Solicitation

Both walls were conditioned at 20 °C and 50% RH for one week before applying the temperature cycles. The outer face of both walls was then exposed to a periodic variation

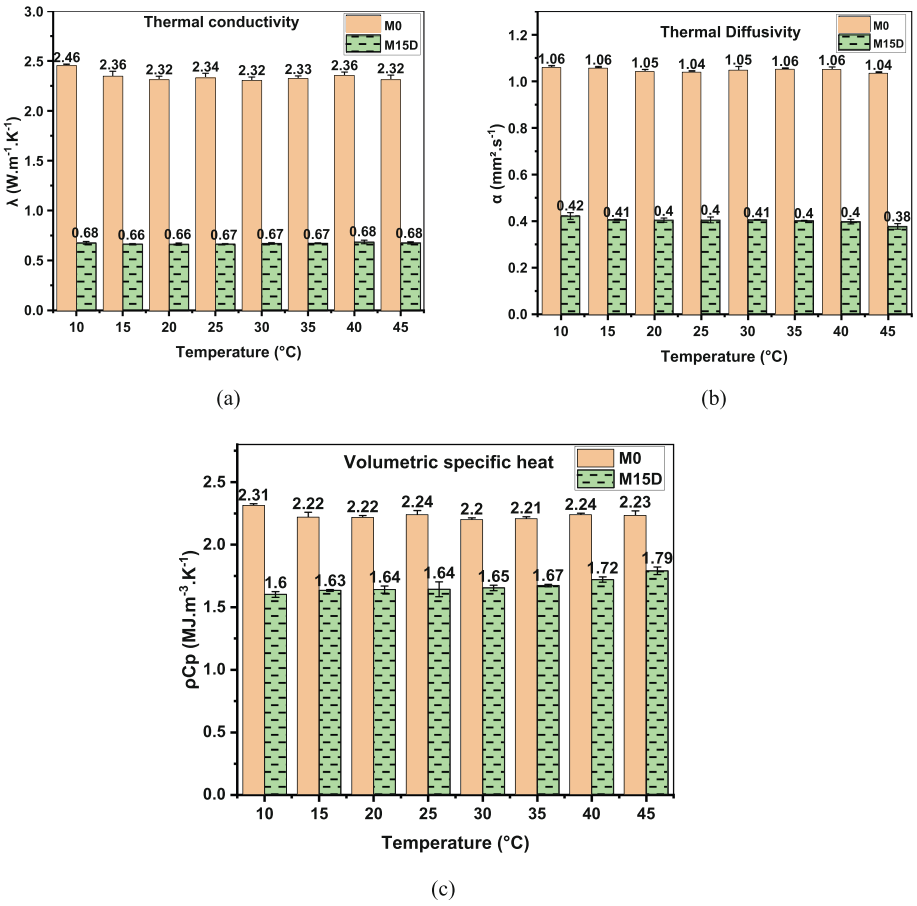

Fig. 4. Thermophysical properties of M0 and M15D determined by the HD method: (a) thermal conductivity, (b) thermal diffusivity, (c) volumetric heat capacity

of temperature (12 h at 40 °C followed by 12 h at 15 °C). This cycle was repeated 3 times to simulate a 3-day exposure, in order to check the repeatability of the response.

Figures 5a and 5b display the responses of the two walls (M0 and M15D) to the dynamic variation of outdoor temperature at a constant RH level of 50%. The temperature profiles obtained at various depths within the walls are shown in the graphs.

For both walls, a good repeatability is obtained between the successive cycles applied for the same boundaries' conditions, which indicate that only one cycle can represent the behavior of each wall. Therefore, a focus on a 24 h cycle with a comparison between the two walls during the heating/cooling process is presented in Fig. 6.

In Fig. 6, the same evolution trends are observed for the temperature profiles of the two walls over a 24 h cycle. During the heating period at 40 °C, the highest temperature recorded by each sensor is obtained at the end of the heating stage. On the outer face of the wall, this maximum temperature is about 35.9 °C for M0 and 34.7 °C for M15D.

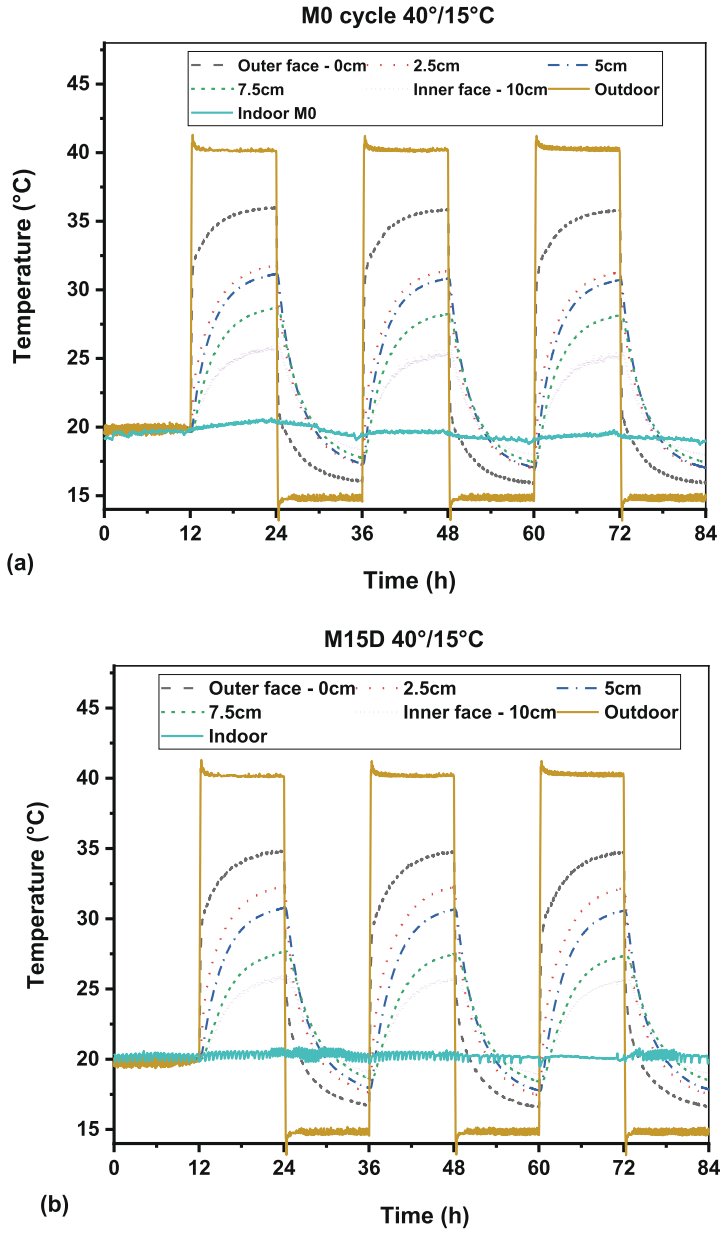

Fig. 5. Responses of the walls to temperature cycles between 40°/15 °C: (a) M0; (b) M15D.

Besides, a gradient of temperature is observed as a function of depth within the two walls, with values decreasing from the outer face to the inner one. Here again, the temperature at a given depth is lower in the M15D wall compared to the reference M0 (with a gap of about 1 °C), except at the depth of 2.5 cm which may result from an error on

the position of the corresponding sensors. This gap of ~1 °C between the two walls may reflect the influence of the mPCMs contained in the M15D wall: as temperature increases over the melting point of mPCMs (~28 °C), the core of mPCM particles becomes liquid and some energy is stored in the form latent heat. This phenomenon may slightly reduce the heating kinetics in the M15D wall. Another interesting feature is that this gap of 1 °C is not observed near the inner face of the walls exposed to the indoor laboratory condition at 20 °C. As the local temperature is below the melting transition of mPCMs, the thermal energy storage process is not activated in this case.

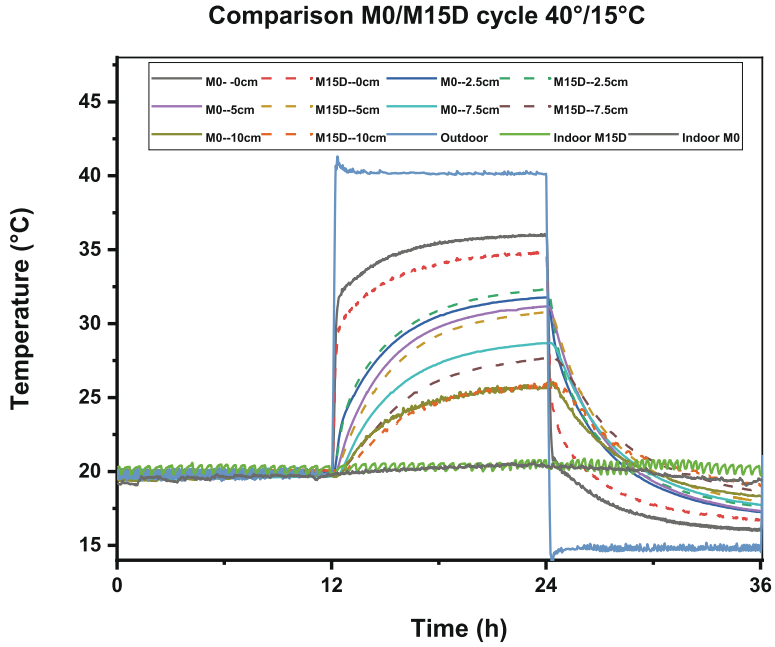

Fig. 6. Compared responses of M0 and M15D walls exposed to a 24 h cycle at 40°/15 °C.

During the cooling stage (12 h at 15 °C), a reverse effect is observed for the temperature gradient evolution. Indeed, the highest temperature is recorded on the inner face (exposed to laboratory condition at 20 °C) and is about 18.3 °C for M0 (19 °C for M15D) and the outer face exhibits the lowest temperature with 15.9 °C for M0 (and 16.8 °C for M15D). The gap of ~1 °C is observed again between the two walls, as M15D exhibits higher temperature than M0 at all depths. Here again, this phenomenon may reflect the influence of the mPCMs: as the temperatures decreases below the crystallization point of mPCMs, a solidification of the PCM core occurs and the stored energy is released, which may dampen the cooling kinetics in M15D compared to M0.

Overall, the damping effect can be evaluated to ~2 °C on the peak-to-peak amplitude during the entire cycle (including both heating and cooling phases).

3.3 Comparison of the Walls' Behaviors Under Steady-State Heating at 40 °C

Figure 7 displays the temperature profiles recorded at various depths within the two walls, when exposed to the second scenario on outdoor conditions (step change from 20 °C to 40 °C followed by a prolonged exposure at 40 °C until steady-state).

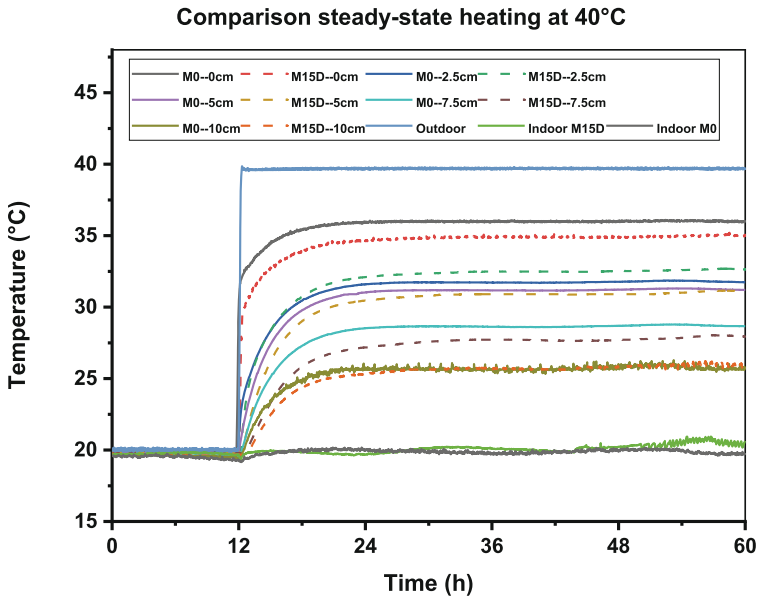

Fig. 7. Comparison between M0 and M15D for a steady-state regime at 40 °C

The temperatures measured at the various depths within the walls increase rapidly after the step change in outdoor temperature from 20 °C to 40 °C; then the evolution kinetics progressively decreases, and a steady-state is reached after about 15 h. As previously observed for scenario 1, the maximum temperature value is recorded on the outer faces of the walls and is about 36 °C for M0 and 35 °C for M15D. A gradient of temperature is also observed as a function of depth in each wall, decreasing from the outer to the inner face. The gap of ~1 °C between the two walls is again observed at depths of 5 cm and 7.5 cm, and can still be attributed to the action of mPCMs contained in M15D. As temperature increases locally over the melting point, the core of mPCM particles becomes liquid, latent heat is stored, and the heating kinetics is slightly decreased.

For the two walls, temperatures measured on the inner faces exposed to the laboratory condition at 20 °C are again almost similar (value of about 25 °C). In this case, the heat storage process of mPCMs is not activated, as local temperature remains below the melting point of the PCM core.

Overall, previous results show that the introduction of mPCMs in the mortar makes it possible to dampen temperature variations in the wall, but only with a limited effect

(damping of ~2 °C on peak-to-peak amplitude during cyclic variation of outdoor temperature between 40 °C/15 °C). One could expect a much stronger effect, since thermophysical properties of the two mortar formulations are very different, especially thermal conductivity (2.32 $W.m^{-1} \cdot K^{-1}$ for M0 and 0.66 $W.m^{-1} \cdot K^{-1}$ for M15D at 20 °C).

Therefore, it may be interesting to conduct complementary investigations by considering alternative scenarios for the variation of the outdoor conditions, or by using specific sensors (to assess the total heat flux across the wall, or the power delivered during heating/cooling phases). Furthermore, finite element (FE) modeling of heat and mass transfer through the two walls could also provide additional information.

4 Conclusion

This study explores the effect of the incorporation of a bio-based and formaldehyde-free mPCMs on the thermal performance of a mortar wall (M15D), compared to a reference wall made of regular mortar (M0). The thermal responses of these walls subjected to two types of dynamic solicitations on a home-made setup were investigated.

During the day/night cyclic loading as well as in a steady-state scenario, the evolutions of temperature gradients exhibit the same trends in both walls. Nevertheless, a gap of about 1 °C is noticed between the walls during the heating phases (and during the cooling phases as well), both on the external face subjected to the outdoor condition and at several depths. Indeed, the incorporation of mPCMs seems to induce a slight damping effect of the temperature variations, due to the energy storage process by latent heat. This damping effect is not observed on the inner face of the M15D wall, as the indoor temperature is below the melting point of the mPCMs and does not allow to activate the heat storage capacity.

It could be interesting to perform additional experiments by applying alternative dynamic scenarios or using flux sensors, and to conduct FE modeling of the heat transfer process, in order to better understand the global thermal behavior of the walls.

Acknowledgement. The authors would like to acknowledge the Labex MMCD (Multi-Scale Modelling & Experimentation of Materials for Sustainable Construction) for its financial support through ANR Investments for the Future (program ANR-11-LABX-022-01).

References

1. Yüksek, I., Karadayi, T.T.: Energy-efficient building design in the context of building life cycle. IntechOpen (2017)
2. Service des données et études statistiques. Bilan énergétique de la France en 2021 - Données provisoires (2022)
3. Chel, A., Kaushik, G.: Renewable energy technologies for sustainable development of energy efficient building. Alex. Eng. J. **57**, 655–669 (2018). https://doi.org/10.1016/j.aej.2017.02.027
4. Amziane, S., Sonebi, M.: Overview on biobased building material made with plant aggregate. RILEM Tech. Lett. **1**, 31–38 (2016). https://doi.org/10.21809/rilemtechlett.2016.9
5. Tyagi, V.V., Buddhi, D.: PCM thermal storage in buildings: a state of art. Renew. Sustain. Energy Rev. **11**, 1146–1166 (2007). https://doi.org/10.1016/j.rser.2005.10.002

6. Kalnæs, S.E., Jelle, B.P.: Phase change materials and products for building applications: a state-of-the-art review and future research opportunities. Energy Build. **94**, 150–176 (2015). https://doi.org/10.1016/j.enbuild.2015.02.023
7. Sarbu, I., Sebarchievici, C.: A comprehensive review of thermal energy storage. Sustainability **10**, 191 (2018). https://doi.org/10.3390/su10010191
8. Sharma, A., Tyagi, V.V., Chen, C.R., Buddhi, D.: Review on thermal energy storage with phase change materials and applications. Renew. Sustain. Energy Rev. **13**, 318–345 (2009). https://doi.org/10.1016/j.rser.2007.10.005
9. Cabeza, L.F., Castell, A., Barreneche, C., de Gracia, A., Fernández, A.I.: Materials used as PCM in thermal energy storage in buildings: a review. Renew. Sustain. Energy Rev. **15**, 1675–1695 (2011). https://doi.org/10.1016/j.rser.2010.11.018
10. Giro-Paloma, J., Martínez, M., Cabeza, L.F., Fernández, A.I.: Types, methods, techniques, and applications for microencapsulated phase change materials (MPCM): a review. Renew. Sustain. Energy Rev. **53**, 1059–1075 (2016). https://doi.org/10.1016/j.rser.2015.09.040
11. Gbekou, F.K., Benzarti, K., Boudenne, A., Eddhahak, A., Duc, M.: Mechanical and thermo-physical properties of cement mortars including bio-based microencapsulated phase change materials. Constr. Build. Mater. **352**, 129056 (2022). https://doi.org/10.1016/j.conbuildmat.2022.129056
12. Das, R., Siva Ranjani Gandhi, I., Muthukumar, P.: Use of agglomerated Micro-encapsulated phase change material in cement mortar as thermal energy storage material for buildings. Mater. Today Proc. **65**, 808–814 (2022). https://doi.org/10.1016/j.matpr.2022.03.316
13. Dehmous, M., Franquet, E., Lamrous, N.: Mechanical and thermal characterizations of various thermal energy storage concretes including low-cost bio-sourced PCM. Energy Build. **241**, 110878 (2021). https://doi.org/10.1016/j.enbuild.2021.110878
14. Lecompte, T., Le Bideau, P., Glouannec, P., Nortershauser, D., Le Masson, S.: Mechanical and thermo-physical behaviour of concretes and mortars containing phase change material. Energy Build. **94**, 52–60 (2015). https://doi.org/10.1016/j.enbuild.2015.02.044
15. Li, Q., et al.: Thermal performance and economy of PCM foamed cement walls for buildings in different climate zones. Energy Build. **277**, 112470 (2022). https://doi.org/10.1016/j.enbuild.2022.112470
16. Khalil, N., Aouad, G., El Cheikh, K., Rémond, S.: Use of calcium sulfoaluminate cements for setting control of 3D-printing mortars. Constr. Build. Mater. **157**, 382–391 (2017). https://doi.org/10.1016/j.conbuildmat.2017.09.109
17. Croda. CrodaTherm^{TM} ME29P: Microencapsulated ambient temperature phase change material, technical datasheet (2018). https://www.crodaindustrialspecialties.com/en-gb/product-finder/product/1381-crodatherm_1_me_1_29d
18. Dehdezi, P.K., Hall, M.R., Dawson, A.R., Casey, S.P.: Thermal, mechanical and microstructural analysis of concrete containing microencapsulated phase change materials. Int. J. Pavement Eng. **14**, 449–462 (2013). https://doi.org/10.1080/10298436.2012.716837
19. Hunger, M., Entrop, A.G., Mandilaras, I., Brouwers, H.J.H., Founti, M.: The behavior of self-compacting concrete containing micro-encapsulated Phase Change Materials. Cement Concr. Compos. **31**, 731–743 (2009). https://doi.org/10.1016/j.cemconcomp.2009.08.002
20. Jayalath, A., et al.: Properties of cementitious mortar and concrete containing micro-encapsulated phase change materials. Constr. Build. Mater. **120**, 408–417 (2016). https://doi.org/10.1016/j.conbuildmat.2016.05.116